JSR Publications

Available Online

J. Sci. Res. **16** (1), 331-342 (2024)

JOURNAL OF SCIENTIFIC RESEARCH

www.banglajol.info/index.php/JSR

Glucose Functionalized Magnetic Iron Oxide Nanoparticles for Protein Detection and Separation

SK. Basiruddin*

Government General Degree College, Tehatta, Nadia-741160, West Bengal, India

Received 30 August 2023, accepted in final revised form 15 October 2023

Abstract

Iron oxide magnetic nanoparticles (MNP) are considered to be emergent nanoparticles for magnetic separation and MRI imaging probes. Here, glucose-functionalized iron oxide (γ-Fe_2O_3) magnetic nanoparticles have been prepared for specific protein detection and separation. First, hydrophobic iron oxide (γ-Fe_2O_3) was synthesized by standard organometallic approaches, and the same has been converted to soluble, colloidally stable, hydrophilic primary amine (-NH_2)-PEG terminated iron oxide (γ-Fe_2O_3) nanoparticles using reverse micelle based robust polyacrylate coating chemistry. Then, glucose was covalently linked to this amine (-NH_2)-PEG terminated iron oxide (γ-Fe_2O_3) nanoparticles by using glutaraldehyde-based coupling chemistry. Finally, glucose-functionalized iron oxide (γ-Fe_2O_3) nanoparticles have been used for specific detection and separation of a glycoprotein, Concanavalin-A.

Keywords: Magnetic Nanoparticle (MNP); Polyacrylate coating; Functionalization; Glucose, Glycoprotein; Concanavalin- A; Detection and separation.

doi: http://dx.doi.org/10.3329/jsr.v16i1.68491 J. Sci. Res. **16** (1), 331-342 (2024)

1. Introduction

Iron oxide nanoparticles are considered emergent in the scientific community due to their potential biomedical applications arising from their biocompatibility and non-toxicity [1]. The superparamagnetic nature of iron oxide nanoparticles allows them to be potentially used in magnetic separation, drug delivery, magnetic resonance imaging (MRI), and hyperthermia of cancer cells [2-5]. However, preparing high-quality and properly engineered magnetic iron oxide nanoparticles is challenging for biomedical applications. We know that in any biomedical application of nanoparticles, nanoparticles need to be hydrophilic and colloidally stable at various pH over a period of time. Therefore, to fulfill these criteria, water-soluble nanoparticles and proper functional groups on the nanoparticle's surface are necessary [5-10]. As we know, most of the powerful synthetic methods produce high-quality nanoparticles capped with hydrophobic fatty acids or amines, making the nanoparticles hydrophobic. Hence, these particles are water-insoluble; at the same time, they are not functionalized with proper groups [11-16]. Proper

* *Corresponding author*: sk.basi@gmail.com

functional groups on the nanoparticle's surface are necessary for linking desired biomolecules using various conjugations chemistry.

On the other hand, functional groups help nanoparticles to get colloidally stable in the biological medium and retain their individual properties. Therefore, the conversion of hydrophobic nanoparticles to hydrophilic nanoparticles is very challenging for the application of functionalized nanoparticles in biological fields. Most researchers used thiol-based molecules to stabilize and functionalize nanoparticles [6-9,17,18]. However, the weak interaction between the stabilizer and nanoparticle surface often leads to colloidal stability issues, especially in biological media in the presence of protein, as proteins have different functional groups with multivalent interactions with the nanoparticles. Functionalizing desired biomolecules to the surface of the nanoparticles is a crucial step for the specific application of functionalized nanoparticles in various biomedical fields [18]. Among the biomolecules, carbohydrates are essential and emerging as carbohydrate-functionalized nanoparticles have been used in different fields of biological science [19-21]. In earlier studies, various scientific communities conjugated carbohydrate molecules with nanoparticles using different conjugation chemistry, for example, adsorption of thiolated carbohydrates with nanoparticles via affinity-based interaction [22–26] or linking of carbohydrates via EDC/ DSC/DCC-based conjugation chemistry with nanoparticles [27–29], click chemistry [30,31], reductive amination based conjugation chemistry [32–35] and other methods [36-38].

This paper uses acrylate-based robust coating chemistry to prepare water-soluble hydrophilic nanoparticles from hydrophobic nanoparticles. This type of coating chemistry not only protects nanoparticles from adverse experimental conditions but also provides better colloidal stability [39]. On top of that, it also provides a thin, crosslinked coating that could protect the core nanoparticle, improve colloidal stability, and introduce chemical functionality for bio-conjugation. Here, we have prepared glucose functionalized γ-Fe_2O_3 iron oxide (γ-Fe_2O_3-glucose) magnetic nanoparticle (MNP) to detect model protein Conconavalin-A. First, hydrophobic iron oxide (γ-Fe_2O_3) magnetic nanoparticle (MNP) was synthesized by standard organometallic approaches; then we converted high-quality hydrophobic γ-Fe_2O_3 nanoparticles into polyacrylate coated hydrophilic water-soluble γ-Fe_2O_3 nanoparticles in such a way primary amine (-NH_2) groups and polyethylene glycol (PEG) groups are terminated on the nanoparticles' surface using our previously reported reverse micelle based polyacrylate coating [40]. This polyacrylate crosslinking coating imparts good colloidal stability to γ-Fe_2O_3 nanoparticles at biological pH (7.4). The primary amine (-NH_2) group on the nanoparticle's surface has been used to link glucosamine by glutaraldehyde-based coupling [41]. PEG groups on the nanoparticles' surface prevent non-specific interactions with the biomolecules as nanoparticles are positively charged (-NH_2 groups). Finally, glucose functionalized γ-Fe_2O_3 MNP have been used to detect and separate glycoprotein Concanavalin- A (Con-A) as Con-A has a specific affinity with glucose molecules. Upon addition of Con-A solution to glucose functionalized γ-Fe_2O_3 nanoparticles solution, particle aggregation or precipitation was noticed, and this particle aggregation or precipitation was separated by a

strong magnetic bar. The interaction between glucose functionalized γ-Fe_2O_3 nanoparticles and Con-A is specific and selective. If it is not a specific interaction, glucose functionalized γ-Fe_2O_3 nanoparticles would have interacted nonspecifically with any glycoprotein. However, it was not observed because we also conducted a set of control experiments between glucose functionalized γ-Fe_2O_3 nanoparticles and bovine serum albumin (BSA) and that of between polyacrylate coated γ-Fe_2O_3 nanoparticles and Con-A as well. However, no such precipitation occurred as found in the earlier case.

2. Experimental

2.1. *Chemicals and reagents*

Octadecyl amine, methyl morpholine N-oxide (MNO), octadecene, D-glucosamine, glutaraldehyde, Igepal CO-520, poly(ethylene glycol) methacrylate (Mn~ 360), N, N′-methylene bisacrylamide, ammonium persulfate, sodium borohydride [$NaBH_4$], dialysis membrane (MWCO 12–14 kDa), concanavalin A (Con A) and bovine serum albumin (BSA) were purchased from Sigma-Aldrich and used as received. N-(3-Aminopropyl)-methacrylamide hydrochloride was purchased from Polysciences, and N,N,N′,N′-tetramethylethylenediamine was purchased from Alfa Aesar.

2.2. *Synthesis of hydrophobic γ-Fe_2O_3 magnetic nanoparticles (MNP)*

Hydrophobic γ-Fe_2O_3 nanoparticles are synthesized by standard organometallic approaches reported earlier [16,42]. First, typically 373 mg of Fe (III) stearate, 160 mg of octadecyl amine, and 160 mg of methyl morpholine N-oxide were taken together in a three-necked flask, and 10 mL of octadecene solvent (having high boiling point hydrophobic solvent) was added to the reaction mixture. Then, the whole mixture was degassed for 15 min with N_2 gas to make the mixture an O_2-free atmosphere. After that, the temperature of the solution was increased gradually to 300 °C. In this condition, the solution was kept for 15 min under N_2 atmosphere to completely form γ-Fe_2O_3. Next, the solution temperature was cooled to room temperature slowly, and finally, synthesized hydrophobic γ-Fe_2O_3 MNP were stored as a stock solution for further use.

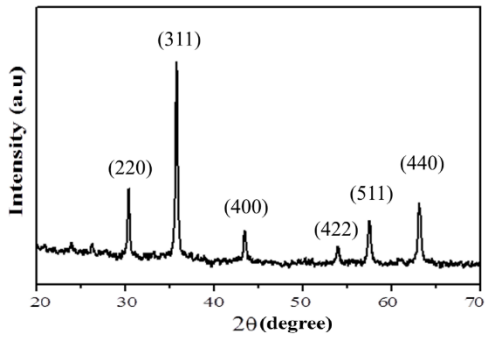

Fig. 1. XRD pattern of as synthesized hydrophobic γ-Fe_2O_3 MNP.

2.3. *Preparation of primary amine terminated iron oxide (γ-Fe_2O_3) nanoparticles via reverse micelle-based polyacrylate coating*

Hydrophobic γ-Fe_2O_3 iron oxide nanoparticles, synthesized by the above method, need to be converted to hydrophilic γ-Fe_2O_3 iron oxide nanoparticles for biological application. That's why these hydrophobic particles were converted into polyacrylate-coated water-soluble nanoparticles using a reverse micelle-based approach reported earlier (Scheme 1) [2,39]. In a typical synthesis, hydrophobic nanoparticles were dissolved in reverse micelles, mixed with the desired acrylate monomers or monomer's mixture, and polymerization was initiated in a nitrogen atmosphere by a persulfate initiator. Here, we have used three acrylates; N-(3-aminopropyl)-methacrylamide that provides a primary amine and a cationic surface charge, poly (ethylene glycol) methacrylate that provides a PEGylated surface into the polyacrylate backbone of coating of iron oxide nanoparticles' surface. Here, 5-mole percent methylene bisacrylamide, with respect to total monomers used, was used to crosslink the polyacrylate shell for better stability of the coating. Typically, 12 mL of Igepal-cyclohexane reverse micelle solution was prepared by mixing 3 mL of Igepal with 9 mL of cyclohexane. Here, cyclohexane is used as a solvent. Then, all the monomer solutions were prepared in three different 2 mL microcentrifuge tubes using this reverse micelle solution. First, 24 mg of N-(3-aminopropyl) acrylamide, 36 μL of poly(ethylene glycol) methacrylate, and 3 mg of N,N′-methylenebisacrylamide were taken in three different 2 mL microcentrifuge tube and all the monomers were dissolved in 100-200 μL of H_2O by handshaking. Then, 1.9 mL of Igepal-cyclohexane reverse micelle solution was added to each microcentrifuge tube, and all the microcentrifuge tubes containing monomers and reverse micelle were shaken vigorously to make solutions optically clear. Next, all three monomer solutions were transferred into a three-necked flask, and the remaining Igepal-cyclohexane reverse micelle solution was added further. After that, hydrophobic iron oxide (γ-Fe_2O_3) solution was added to the reverse micelle monomeric reaction mixture, followed by the addition of 100 μL of N,N,N′,N′-tetramethylethylenediamine to make the reaction medium basic. The reaction mixture needs to be made O_2-free as O_2 prevents the acrylate polymerization process. That's why

the reaction mixture was kept in a magnetically stirring condition and purged with nitrogen for ~15 min to make the reaction mixture O_2-free. Then, the initiator, ammonium persulfate (APS) solution (3 mg dissolved in 100 µL of H_2O) was added to initiate the polymerization process. The reaction was continued for 1 h in an N_2 atmosphere and magnetically stirring condition. After that, the polyacrylate coating was quenched by the addition of a small amount of ethanol and disconnected from the N_2 gas source. After one hour of reaction, the polyacrylate-coated γ-Fe_2O_3 iron oxide magnetic nanoparticles were separated by ethanol addition, washed thoroughly with chloroform, and finally dissolved in water. The resultant polymer-coated γ-Fe_2O_3 iron oxide nanoparticles were terminated with primary amine and PEG, respectively, on the nanoparticles' surface.

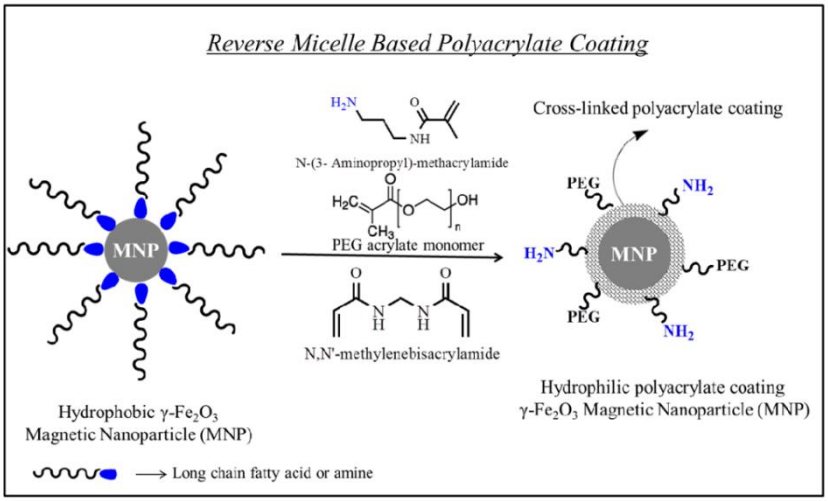

Scheme 1. Schematic conversion of hydrophobic γ-Fe_2O_3 MNP to primary amine and PEG terminated polyacrylate coated iron oxide (γ-Fe_2O_3) MNP.

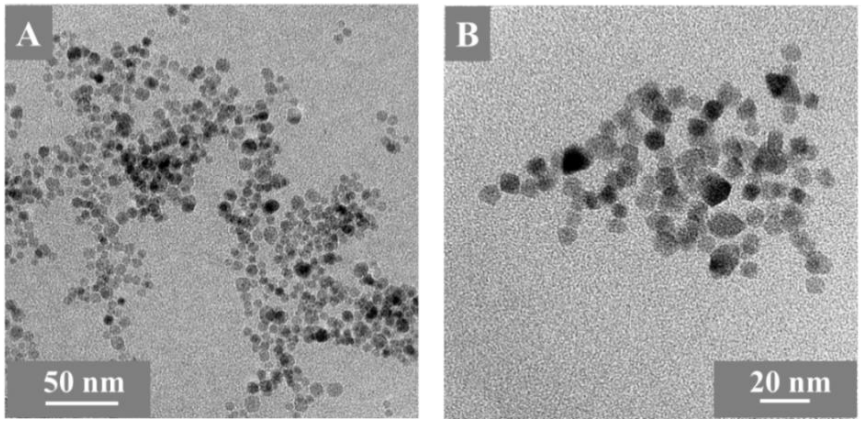

Fig. 2. TEM images of synthesized hydrophobic γ-Fe_2O_3 MNP (A) and polyacrylate coated water soluble iron oxide (γ-Fe_2O_3) MNP (B).

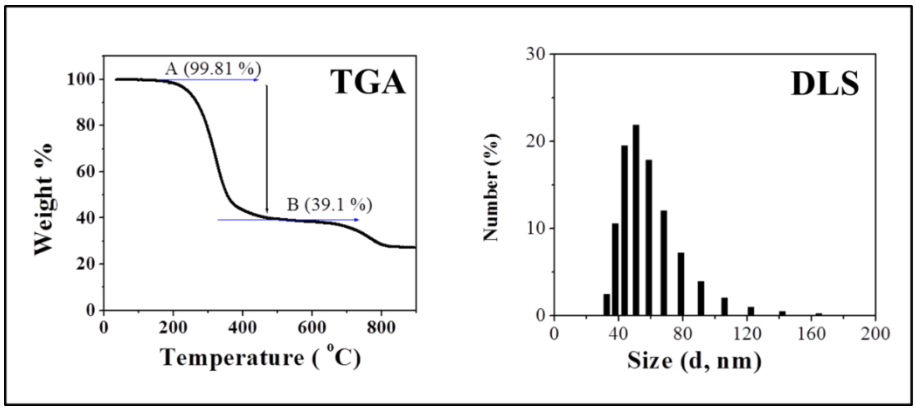

Fig. 3. Thermogravimetry analysis (TGA) and dynamic light scattering (DLS) studies of polyacrylate coated γ-Fe_2O_3 MNP.

2.4. *Glucose functionalization of amine-PEG terminated iron oxide (γ-Fe_2O_3) MNP*

Glucose functionalization of amine and PEG terminated γ-Fe_2O_3 nanoparticles was carried out by glutaraldehyde-based coupling (Scheme 2). Glucose conjugation with amine-terminated iron oxide (γ-Fe_2O_3-NH_2) was performed in 0.1 M carbonate buffer of pH 10.0. First, 0.01 mM glucosamine was mixed with equivalent glutaraldehyde in 0.5 mL of aqueous carbonate buffer solution. After 15 min of mixing, 100-200 μL of this solution was mixed with 1-2 mL of polymer-coated amine-terminated iron oxide (γ-Fe_2O_3) solution. After 1 h, this solution was mixed with 200 μL of $NaBH_4$ (0.2 M) solution to reduce the imine bonds formed by the reaction between aldehyde and amine. After overnight, this solution was dialyzed overnight at 4 °C against deionized water using 12-14 kDa molecular weight cutoff (MWCO) membranes to remove unbound glucosamine and other reagents. Finally, this glucose-functionalized iron oxide (γ-Fe_2O_3) was mixed with a phosphate buffer of pH 7.5 and preserved at 4 °C.

2.5. *Protein detection using glucose-functionalized iron oxide (γ-Fe_2O_3) MNP*

Protein detection tests of glucose-functionalized iron oxide (γ-Fe_2O_3) nanoparticles were performed in 0.02 M phosphate buffer of pH 7.5. Here, we have taken concanavalin A as a model protein. As polyacrylate γ-Fe_2O_3 magnetic nanoparticles have no specific absorbance peak (λ_{max}) in the UV-visible spectra, for the protein detection experiment, 0.26 absorbance at 450 nm was taken as the concentration of the polyacrylate coated γ-Fe_2O_3 or glucose functionalized γ-Fe_2O_3 nanoparticles (Fig. 4). The glucose functionalized iron oxide (γ-Fe_2O_3) nanoparticles were taken in a UV cuvette in phosphate buffer solution. Next, 100 μL (i.e., 5 μM) of the concanavalin-A solution was added to the UV cuvette. In control experiments, 5 μM BSA solution was used instead of concanavalin-A. In other control experiments, only polymer-coated iron oxide (γ-Fe_2O_3)

nanoparticles (without glucose functionalization) were used and mixed with concanavalin-A solution (5 μM)). No particle aggregation was observed in these control experiments (Figs. 5b and 5c). Only the selective binding of protein with glucose-functionalized iron oxide (γ-Fe_2O_3) nanoparticles leads to nanoparticle aggregation, observed by visible precipitation of particles. Finally, MNP aggregation, produced due to the interaction between glucose-functionalized iron oxide (γ-Fe_2O_3) nanoparticles and Concanavalin-A, was separated by a magnet (Fig. 5a).

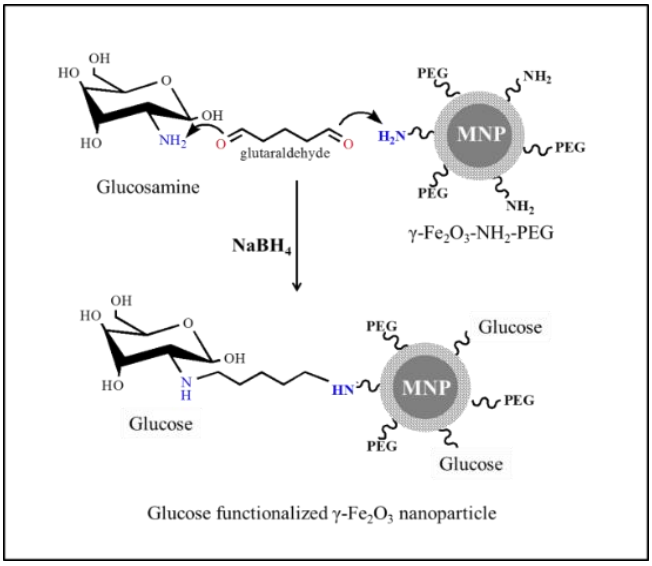

Scheme 2. Glucose functionalization of amine-terminated γ-Fe_2O_3 MNP by glutaraldehyde-based coupling.

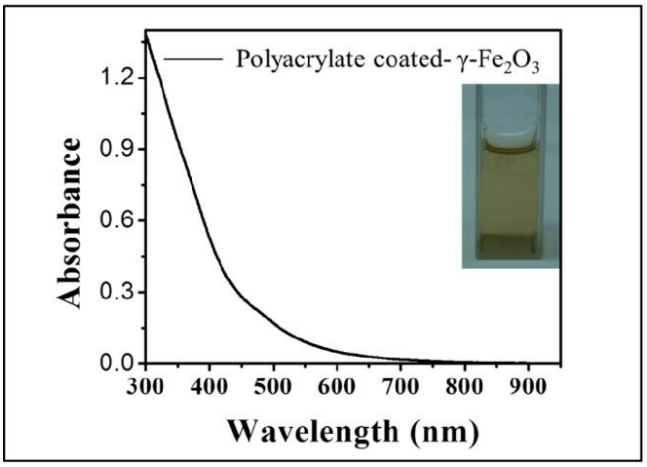

Fig. 4. UV-visible spectra of polyacrylate coated γ-Fe_2O_3 MNP. Digital photo of polyacrylate coated γ-Fe_2O_3 MNP shows good colloidal stability in aqueous solution.

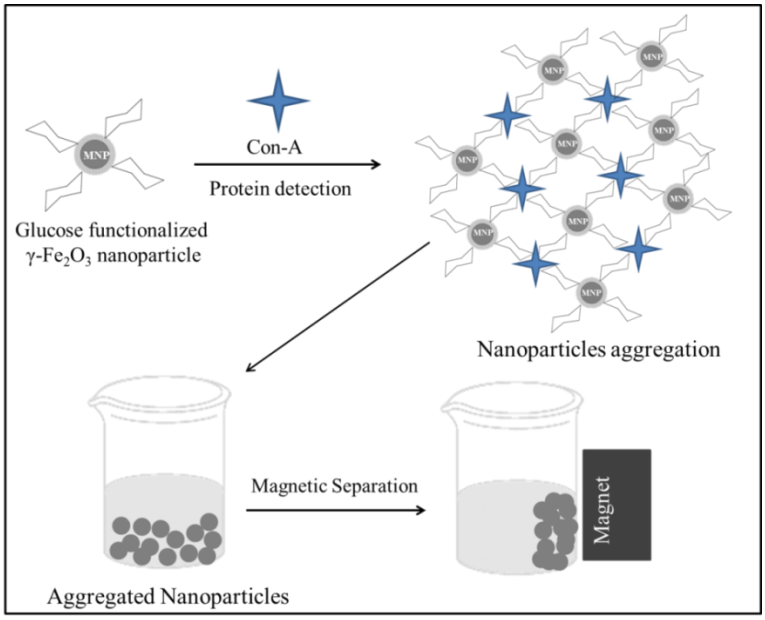

Scheme 3. Schematic representation of Con-A protein detection and separation by glucose functionalized iron oxide (γ-Fe_2O_3) MNP.

3. Results and Discussion

As synthesized, the high-quality nanoparticle is generally capped with long-chain fatty acids (oleic acid/stearic acid) or amines (octadecyl amine/oleylamine), which make them hydrophobic. Here, hydrophobic γ-Fe_2O_3 MNP were synthesized by standard organometallic approaches. Fig. 1 shows the XRD pattern of synthesized hydrophobic γ-Fe_2O_3. It shows the reflection at 30, 36, 43, 54, 57, and 63° corresponding to the plane of (220), (311), (400), (422), (511) and (440) of γ-Fe_2O_3 nanoparticles. These hydrophobic nanoparticles need to be converted to hydrophilic water-soluble nanoparticles for biomedical applications. Polyacrylate-based robust coating chemistry has been used to convert synthesized hydrophobic iron oxide (γ-Fe_2O_3) MNP to hydrophilic nanoparticles. Reverse micelle-based crosslinking polymer polyacrylate coating produced primary amine, and PEG terminated γ-Fe_2O_3 iron oxide nanoparticles from hydrophobic nanoparticles (Scheme 1). Here, we have used three acrylates: N-(3-aminopropyl)-methacrylamide that provides a primary amine and a cationic surface charge, poly (ethylene glycol) methacrylate that provides a PEGylated surface into the polyacrylate backbone of coating of iron oxide nanoparticles' surface. Here, 5-mole percent methylene bisacrylamide, with respect to total monomers used, was used to crosslink the polyacrylate shell for better stability of the coating. The TEM image (Fig. 2a) shows the size of the synthesized hydrophobic γ-Fe_2O_3 in the order of~ 12-15 nm. Polyacrylate coating on the nanoparticle is not seen in the TEM image as it is composed of monomers of light atoms.

Therefore after polyacrylate coating of γ-Fe_2O_3, the size of the nanoparticles remained same (Fig. 2b). Dynamic light scattering (DLS) study (Fig. 3) of polyacrylate coated γ-Fe_2O_3 shows that polyacrylate coated γ-Fe_2O_3 MNP have good colloidal stability in aqueous medium with hydrodynamic size in the range of ~ (40-60) nm and no precipitate or aggregation was found in aqueous solution as well as corresponding size in the DLS curve. Thermogravimetry analysis (TGA) (Fig. 3) of polyacrylate coated γ-Fe_2O_3 MNP shows that polyacrylate coating on the surface of the nanoparticles undergoes thermal degradation or decomposition (or weight loss) in the temperature range starting from 200 °C to 420 °C and the main weight loss observed around 335 °C. The TGA curve shows that around 60 % of the total weight of polyacrylate-coated γ-Fe_2O_3 is lost due to thermal degradation. Therefore, the TGA study confirms polyacrylate coating on the γ-Fe_2O_3 MNP surface.

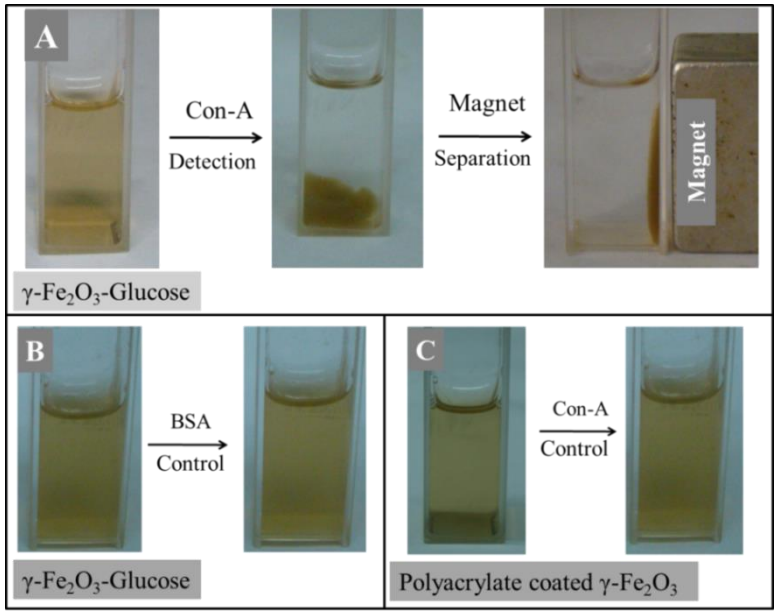

Fig. 5. Pictures **A** shows the specific detection of Con-A protein using glucose-functionalized iron oxide (γ-Fe_2O_3) MNP, while pictures **B** and **C** show the control experiments. (See details in the result and discussion section).

Then, in order to bio-functionalize amine and PEG terminated γ-Fe_2O_3 iron oxide MNP, glutaraldehyde-based coupling chemistry has been used (Scheme 2). Here, the nanoparticle's surface's primary amine groups (-NH_2) are used to covalently link glucosamine by glutaraldehyde-based coupling chemistry. As we know, glutaraldehyde has two –CHO groups at the two ends. Hence, the -NH_2 group of glucosamine reacts with one aldehyde group of glutaraldehyde, and another aldehyde group reacts with -NH_2 groups of amine-terminated γ-Fe_2O_3 nanoparticles through reductive imine-based coupling chemistry. In this fashion, many glucosamine molecules are liked with amine, and PEG

terminated γ-Fe_2O_3 nanoparticles surface. Finally, imine groups are reduced by $NaBH_4$ as imine groups are unstable in a water medium. In this way, glucose functionalized iron oxide (γ-Fe_2O_3) MNP have been prepared. Finally, glucose functionalized iron oxide (γ-Fe_2O_3) nanoparticles have been used to detect and separate glycoprotein Concanavalin-A (Con-A). Concanavalin-A is a glycoprotein with four binding sites for glucose molecules, i.e., one Con-A binds four molecules simultaneously. Therefore, upon the addition of Con-A to the solution of glucose-functionalized iron oxide (γ-Fe_2O_3) nanoparticles, glucose molecules of two or more two nanoparticles bind to one Con-A protein and many more simultaneously. As a result, glucose-functionalized iron oxide (γ-Fe_2O_3) nanoparticles get aggregated or precipitated out of the solution (Scheme 3 and Fig. 5a). These glucose-functionalized magnetic nanoparticles, and Con-A aggregates are separated by a strong magnet (Fig. 5a). The interaction between glucose functionalized γ-Fe_2O_3 magnetic nanoparticles, and con-A is specific and selective. Whether this interaction is specific or non-specific was checked by two control experiments, one is between BSA and glucose-functionalized iron oxide (γ-Fe_2O_3) nanoparticles (Fig. 5b) and another is between Con-A and polyacrylate-coated iron oxide (γ-Fe_2O_3) nanoparticles (Fig. 5c). Among these two control experiments, in one control experiment, BSA protein was added to the solution of glucose functionalized iron oxide (γ-Fe_2O_3) nanoparticles and in another control experiment Con-A protein was added to the polyacrylate coated iron oxide (γ-Fe_2O_3) nanoparticles (without glucose functionalization). It was observed that no aggregation or precipitation was found in the cases. If the interaction between Con-A and glucose functionalized iron oxide (γ-Fe_2O_3) nanoparticles was non-specific and only interaction between nanoparticles and mix charged (zwitterion) protein, there would have been aggregation on addition of BSA to the glucose functionalized iron oxide (γ-Fe_2O_3) nanoparticles solution or addition of Con-A to the polyacrylate coated iron oxide (γ-Fe_2O_3) nanoparticles solution because both BSA and Con-A are mix charged (zwitterion) proteins. No such aggregation was observed in these two control experiments, indicating that glucose-functionalized iron oxide (γ-Fe_2O_3) nanoparticles specifically bind to the Con-A glycoprotein and have been used to detect Con-A. A strong magnetic bar is not able to separate the glucose-functionalized iron oxide (γ-Fe_2O_3) magnetic nanoparticles from its aqueous solution as it has good colloidal stability (Fig. 4). When Con-A binds two or more glucose-functionalized iron oxide (γ-Fe_2O_3) MNP simultaneously at a time, it produces nanoparticles aggregation, then these aggregates are separated by a strong magnetic bar (Fig. 5a) easily. In this study, glucose-functionalized iron oxide (γ-Fe_2O_3) nanoparticles have been used to detect and separate Con-A glycoprotein. Therefore, glucose-functionalized iron oxide (γ-Fe_2O_3) nanoparticles can be used for detection, separation, and labeling as MRI probes for those glycoprotein or macromolecules containing biological entities that have specific affinity with glucose molecules.

4. Conclusion

Glucose functionalized iron oxide (γ-Fe_2O_3) MNP have been synthesized for potential application in protein detection and separation. This bio-probe is highly colloidal stable

over a period of time. This glucose-functionalized iron oxide (γ-Fe_2O_3) MNP can be used for selective separation and MRI imaging probes. As we know, some cancer cells overexpress glucose receptors; hence, this bio probe could also be used in magnetic field-induced targeted drug delivery, MRI imaging, and hyperthermia of cancer cells through glucose-glucose receptor-based interaction.

Acknowledgment

I gratefully acknowledge the Higher Education Department of the Government of West Bengal, India. I sincerely thank N. R. Jana for his support and assistance. I am also thankful to A. Sinha for his help in the XRD study.

References

1. Q. A. Pankhurst, J. Connolly, S. K. Jones, and J. Dobson, J. Phys. D: Appl. Phys. **36**, R167 (2003). https://doi.10.1088/0022-3727/36/13/201
2. S. K. Basiruddin, A. Saha, R. Sarkar, M. Majumder, and N. R. Jana, Nanoscale **2**, 2561 (2010). https://doi.org/10.1039/C0NR00501K
3. T. K. Mandal and V. Patait, J. Sci. Res. **13**, 299 (2021). https://doi.org/10.3329/jsr.v13i1.47690
4. I. Rabias, D. Tsitrouli, E. Karakosta, T. Kehagias et al., Biomicrofluidics **4**, ID 024111 (2010). https://doi.org/10.1063/1.3449089
5. H. B. Na, I. C. Song, and T. Hyeon, Adv. Mater. **21**, 2133 (2009). https://doi.org/10.1002/adma.200802366
6. I. L. Medintz, H. T. Uyeda, E. R. Goldman, and H. Mattoussi, Nat. Mater. **4**, 435 (2005). https://doi.org/10.1038/nmat1390
7. X. Huang, I. H. El-Sayed, W. Qian, and M. A. El-Sayed, J. Am. Chem. Soc. **128**, 2115 (2006). https://doi.org/10.1021/ja057254a
8. M. De, P. S Ghosh, and V. M. Rotello, Adv. Mater. **20**, 4225 (2008). https://doi.org/10.1002/adma.200703183
9. C. J. Murphy, A. M. Gole, J. W. Stone, P. N. Sisco et al., Acc. Chem. Res. **41**, 1721 (2008). https://doi.org/10.1021/ar800035u
10. X. Gao, Y. Cui, R. M. Levenson, L. W. K. Chung, and S. Nie, Nat. Biotechnol. **22**, 969 (2004). https://doi.org/10.1038/nbt994
11. J. J. Li, Y. A. Wang, W. Guo, J. C. Keay et al., J. Am. Chem. Soc. **125**, 12567 (2003). https://doi.org/10.1021/ja0363563
12. N. Pradhan, D. Goorskey, J. Thessing, and X. Peng, J. Am. Chem. Soc. **127**, 17586 (2005). https://doi.org/10.1021/ja055557z
13. C. B. Murray, D. J. Norris, and M. G. Bawendi, J. Am. Chem. Soc. **115**, 8706 (1993). https://doi.org/10.1021/ja00072a025
14. M. Brust, M. Walker, D. Bethell, D. J. Schiffrin, and R. Whyman, Chem. Commun. 801 (1994). https://doi.org/10.1039/C39940000801
15. N. R. Jana and X. *J.* Peng, J. Am. Chem. Soc. **125**, 14280 (2003). https://doi.org/10.1021/ja038219b
16. N. R. Jana, Y. F. Chen, and X. Peng, Chem. Mater. **16**, 3931 (2004). https://doi.org/10.1021/cm049221k
17. N. L. Rosi and C. A. Mirkin, Chem. ReV. **105**, 1547 (2005). https://doi.org/10.1021/cr030067f
18. K. G. Thomas and P. V. Kamat, Acc. Chem. Res. **36**, 888 (2003). https://doi.org/10.1021/ar030030h
19. Y. H. Su, H. C. Lin, H. Y. Li, C. H. Lien, Y. H. Shih, and C. H. Lai, ACS Appl. Nano Mater. **6**, 4957 (2023). https://doi.org/10.1021/acsanm.3c00722

20. J. Hooper, D. Budhadev, D. L. F. Ainaga, N. Hondow, D. Zhou, and Y. Guo, ACS Appl. Nano Mater. **6**, 4201 (2023). https://doi.org/10.1021/acsanm.2c05247
21. S. A. Wijesundera, K. W. Jayawardana, and M. Yan, ACS Appl. Nano Mater. **5**, 10704 (2022). https://doi.org/10.1021/acsanm.2c02047
22. H. Otsuka, Y. Akiyama, Y. Nagasaki, and K. Kataoka, J. Am. Chem. Soc. **123**, 8226 (2001). https://doi.org/10.1021/ja010437m
23. R. Kikkeri, B. Lepenies, A. Adibekian, P. Laurino, and P. H. Seeberger, J. Am. Chem. Soc. **131**, 2110 (2009). https://doi.org/10.1021/ja807711w
24. R. Wilson, D. G. Spiller, A. Beckett, I. A. Prior, and V. See, Chem. Mater. **22**, 6361 (2010). https://doi.org/10.1021/cm1023635
25. M. Yu, Y. Yang, R. C. Han, Q. Zheng et al., Langmuir **26**, 8534 (2010). https://doi.org/10.1021/la904488w
26. T. Ohyanagi, N. Nagahori, K. Shimawaki, H. Hinou, T. Yamashita et al., J. Am. Chem. Soc. **133**, 12507 (2011). https://doi.org/10.1021/ja111201c
27. C. Earhart, N. R. Jana, N. Erathodiyil, and J. Y. Ying, Langmuir **24**, 6215 (2008). https://doi.org/10.1021/la800066g
28. C. H. Lai, C. Y. Lin, H. T. Wu, H. S. Chan, Y. J. Chuang et al., Adv. Funct. Mater. **20**, 3948 (2010). https://doi.org/10.1002/adfm.201000461
29. A. P. Goodwin, S. M. Tabakman, K. Welsher, S. P. Sherlock, G. Prencipe, and H. J. Dai, J. Am. Chem. Soc. **131**, 289 (2009). https://doi.org/10.1021/ja807307e
30. S. Srinivasachari, Y. M. Liu, G. D. Zhang, L. Prevette, and T. M. Reineke, J. Am. Chem. Soc. **128**, 8176 (2006). https://doi.org/10.1021/ja0585580
31. K. El-Boubbou, D. C. Zhu, C. Vasileiou, B. Borhan, D. Prosperi et al., J. Am. Chem. Soc. **132**, 4490 (2010). https://doi.org/10.1021/ja100455c
32. M. Yalpani and D. E. Brooks, J. Polym. Sci. Polym. Chem. Ed. **23**, 1395 (1985). https://doi.org/10.1002/pol.1985.170230513
33. Q. H. Zhao, I. Gottschalk, J. Carlsson, L. E. Arvidsson, S. Oscarsson et al., Bioconjugate Chem. **8**, 927 (1997). https://doi.org/10.1021/bc970173m
34. S. S. Banerjee and D. H. Chen, Chem. Mater. **19**, 6345 (2007). https://doi.org/10.1021/cm702278u
35. J. C. Gildersleeve, O. Oyelaran, J. T. Simpson, and B. Allred, Bioconjugate Chem. **19**, 1485 (2008). https://doi.org/10.1021/bc800153t
36. F. Osaki, T. Kanamori, S. Sando, T. Sera, and Y. Aoyama, J. Am. Chem. Soc. **126**, 6520 (2004). https://doi.org/10.1021/ja048792a
37. T. T. Beaudette, J. A. Cohen, E. M. Bachelder, K. E. Broaders, J. L. Cohen et al., J. Am. Chem. Soc. **131**, 10360 (2009). https://doi.org/10.1021/ja903984s
38. J. Fernandes, T. Vaz, S. M. Gurav, and T. S. Anvekar, J. Sci. Res. **13**, 1043 (2021). https://doi.org/10.3329/jsr.v13i3.53740
39. Y. F. Wei, N. R. Jana, S. J. Tan, and J. Y. Ying, Bioconjugate Chem. **20**, 1752 (2009). https://doi.org/10.1021/bc8003777
40. S. K. Basiruddin, A. Saha, N. Pradhan, and N. R. Jana, Langmuir **26**, 7475 (2010). https://doi.org/10.1021/la904189a
41. A. Saha, S. K. Basiruddin, R. Sarkar, N. Pradhan, and N. R. Jana, J. Phys. Chem. C **113**, 18492 (2009). https://doi.org/10.1021/jp904791h
42. A. Sinha, S. K. Basiruddin, A. Chakraborty, and N. R. Jana, ACS Appl. Mater. Interfaces **7**, 1340 (2015). https://doi.org/10.1021/am507817b